Analysis of the dynamic response of layered, elastic media by means of the Fast Fourier Transform

A.M.A.M. Abdelkarim and A.C.W.M. Vrouwenvelder
Section of Structural Mechanics and Dynamics, Department of Civil Engineering,
Faculty of Civil Engineering and Geosciences, Stevinweg 1, 2628 CN Delft, Netherlands

M.D. Verweij
Laboratory of Electromagnetic Research, Department of Electrical Engineering,
Faculty of Information Technology and Systems, Mekelweg 4, 2628 CD, Delft, Netherlands

A straightforward method is presented to calculate the three-dimensional response of layered, elastic half-spaces to a dynamic surface loading. The derivation of the method is performed in the wave-number-frequency domain. Space-frequency domain results are subsequently obtained through the application of the Fast Fourier Transform. The results show good agreements with the static solutions of Boussinesq and the dynamic solutions of Lamb.

Keywords: **Dynamics, wave propagation, layered media, FFT**

1 Introduction

Review of the literature on wave propagation theory shows that there is a large variety of techniques for solving wave propagation problems in stratified media. One formalism to describe the propagation of waves in layered media has been presented by Thomson (1950) and Haskell (1953). This formalism is based on the use of transfer matrices in the wavenumber-frequency domain, which relate the displacement and stress components at a given interface with those at the other interfaces. The Thomson-Haskel technique may exhibit numerical difficulties at high frequencies, large depths, and a large number of layers. These difficulties are caused by the occurrence in the transfer matrix of both small and large exponential elements, the combination of which gives rise to a loss of significant figures during matrix multiplication.
Dunkin (1965) has avoided these difficulties by using the determinant matrix decomposition theory and by expressing the solution in terms of its Laplace-Fourier transformation. Gilbert and Backus (1966) have given another method, in which a propagator matrix is obtained through matrix polynomial approximations, using the method of mean coefficients as described by the Cayley-Hamilton theorem. Richard, Hall and Woods (1970) and Kennett (1983) have also used the propagator matrix approach. The stiffness matrix approach forms an alternative method that has been presented by Kausel and Roesset (1981). In this method, the external loads that are applied at the

layer interfaces are related to the displacements at these locations through stiffness matrices. The application of this method is restricted to problems involving only simple geometries.
Once the wavenumber-frequency domain solutions for a layered medium have been obtained, the synthesis of the space-frequency domain result or the space-time domain result forms another difficulty. Most of the work that has been done in this area involves mathematical methods such as contour integration, the steepest descent method, the Hankel-Laplace transformation, the Cagniard-de Hoop method, etc. See, for example, Lamb (1904), Cagniard (1939), Ewing , Jardetzky and Press (1957), De Hoop (1960), Haskell (1964), Harkrider (1964), Hudson (1969), Harkrider (1970), Chapman (1978), Kennett (1983), Van der Hijden (1987), De Hoop (1988), Verweij and De Hoop (1990), and Wolf (1985, 1988).
In this paper, we present a method that is both mathematically straightforward and numerically easy to implement. The first aim is to avoid as much mathematical difficulties as possible, so that the method may be understood with only a basic knowledge of the theory of wave propagation. The second aim is to end up with wave field representations that only require commonly available numerical routines for their evaluation.
The solution technique adopted in this publication will be based on expressing the load and the wavefield quantities in terms of their temporal and horizontal spatial Fourier transforms. According to the Helmholtz theory, any vector field can be expressed as the sum of the gradient of a scalar field and the curl of a vector field, see Ewing *et al.* (1957). The displacement vector will thus be decomposed into scalar and vector potentials. Four potential functions, the scalar potential and the three components of the vector potential, then represent the displacement field. Each potential function consists of *two* terms representing waves that propagate in the positive and the negative vertical direction, respectively. Consequently, at this stage the displacement field is described by *eight* functions for each layer. The condition of zero divergence of the vector potential provides *two* conditions, which reduces the problem to solve for *six* functions for each layer. Once these functions are obtained for all the layers, the displacement field is completely determined. For a medium that consists of N parallel layers, the required $6N$ functions will follow from solving $3N$ second-order differential equations, giving $6N$ general solutions. To find the $6N$ constant multipliers, $6N$ restrictions will be imposed. The boundary conditions at the surface of the medium give *three* of these conditions, the continuity of the displacements and stresses across the interfaces between the layers provide $6(N\text{-}1)$ conditions, and the radiation conditions at infinity yield the final *three* conditions.

2 Basic equations and the solution inside the layers

When discussing wave propagation in an elastic medium it is usually convenient to start with the basic concepts of elasticity and the stress-strain relationships. Since these aspects have been well established by many authors, the analysis will start with the elastodynamic equation that governs wave propagation in a homogeneous, isotropic, elastic medium. In the absence of body forces this equation is given by

$$(\lambda + \mu)\nabla\nabla \cdot \boldsymbol{u} + \mu\nabla^2\boldsymbol{u} = \rho\frac{\partial^2 \boldsymbol{u}}{\partial t^2}, \tag{1}$$

where ρ is the volume density of the material, ∇ is the nabla operator of vector calculus, and λ and μ are the Lamé parameters of the material. According to the Helmholtz vector decomposition theorem, the displacement vector field can be expressed as

$$\boldsymbol{u} = \nabla\phi + \nabla \times \Psi, \tag{2}$$

i.e., the vector field $\boldsymbol{u}$ is represented as a sum of the gradient of a scalar potential ϕ and the curl of a vector potential Ψ. The condition $\nabla \cdot \Psi = 0$ provides an additional condition that uniquely determines the three components of Ψ. Substitution of Eq. (2) into Eq. (1) reveals that ϕ and Ψ are the solutions of the wave equations

$$\nabla^2\phi = \frac{1}{c_1^2}\frac{\partial^2\phi}{\partial t^2}, \qquad \text{with} \qquad c_1^2 = (\lambda + 2\mu)/\rho, \tag{3}$$

and

$$\nabla^2\Psi = \frac{1}{c_2^2}\frac{\partial^2\Psi}{\partial t^2}, \qquad \text{with} \qquad c_2^2 = \mu/\rho. \tag{4}$$

In these equations, c_1 is the compressional wave speed, and c_2 is the shear wave speed. The above formulation is discussed in more detail in many works, see for example Ewing *et al.* (1957), and Eringen and Suhubi (1975).

The solution of the problem is conducted in the wavenumber-frequency domain, which is arrived at after performing the temporal Fourier transformation given by

$$f(x, y, z, \omega) = \int_{-\infty}^{\infty} f(x, y, z, t)e^{i\omega t}dt, \tag{5}$$

followed by the horizontal spatial Fourier transformations

$$f(\alpha, \beta, z, \omega) = \int_{-\infty}^{\infty}\int_{-\infty}^{\infty} f(x, y, z, \omega)e^{-i(\alpha x + \beta y)}dxdy. \tag{6}$$

For each individual load component with a harmonic behavior in x, y, and t, the generated waves in the medium can be represented by a scalar potential ϕ and a vector potential Ψ with the corresponding values of the transform parameters α, β, and ω. Now the problem is reduced to finding $\phi(\alpha, \beta, z, \omega)$ and $\Psi(\alpha, \beta, z, \omega)$ from the second-order, ordinary differential equations that result after the transformation of Eqs. (3) and (4). In the following analysis, the arguments of the functions in the wavenumber-frequency domain will be suppressed. We can express the solutions of the transformed wave equations as

$$\phi = (\bar{T}_1 e^{i\xi z} + \bar{R}_1 e^{-i\xi z}) e^{i(\alpha x + \beta y - \omega t)}, \tag{7}$$

$$\Psi_x = (\bar{T}_2 e^{i\zeta z} + \bar{R}_2 e^{-i\zeta z}) e^{i(\alpha x + \beta y - \omega t)}, \tag{8}$$

$$\Psi_y = (\bar{T}_3 e^{i\zeta z} + \bar{R}_3 e^{-i\zeta z}) e^{i(\alpha x + \beta y - \omega t)}, \tag{9}$$

$$\Psi_z = \left[\left(\frac{-\alpha}{\zeta}\bar{T}_2 + \frac{\beta}{\zeta}\bar{T}_3\right) e^{i\zeta z} + \left(\frac{\alpha}{\zeta}\bar{R}_2 + \frac{\beta}{\zeta}\bar{R}_3\right) e^{-i\zeta z}\right] e^{i(\alpha x + \beta y - \omega t)} \tag{10}$$

To obtain the last equation, the condition $\nabla \cdot \Psi = 0$ has been used. In Eqs. (7) – (10), we have introduced the vertical slownesses ξ and ζ as the square roots of

$$\xi^2 = k_1^2 - \alpha^2 - \beta^2, \qquad \text{with} \qquad k_1^2 = \omega^2 / c_1^2, \tag{11}$$

and

$$\zeta^2 = k_2^2 - \alpha^2 - \beta^2, \qquad \text{with} \qquad k_2^2 = \omega^2 / c_2^2, \tag{12}$$

respectively. To make these vertical slownesses single-valued we require that $\mathrm{Im}[\xi] \geq 0$ and $\mathrm{Im}[\zeta] \geq 0$. This implies that terms with the factors $e^{i\xi z}$ and $e^{i\zeta z}$ represent waves propagating in the positive z-direction (downward), while terms with the factors $e^{-i\xi z}$ and $e^{-i\zeta z}$ represent waves propagating in the negative z-direction (upward).

3 Transmission and reflection of waves at the interfaces

In each layer, the unknown coefficients $\bar{T}_i$ and $\bar{R}_i$ ($i = 1,2,3$) determine the amplitudes of the potential functions. These amplitudes change at the layer interfaces, depending on the transmission and reflection of the waves at these locations. Thus, the evaluation of the wave field in a layered medium that consists of N elastic layers in contact, reduces to the determination of $6N$ unknown amplitudes. These are found from $6N$ restrictions. As we will see, a simple recurrence scheme may be obtained for the generation of the transmission and reflection coefficients in the layered medium. Consider a layered elastic half-space ($z \geq 0$) consisting of N-1 parallel, horizontal layers overlaying a uniform half-space called layer N. The jth layer ($j = 1,\ldots,N$-1) is bounded by upper and lower interfaces located at depths z_{j-1} and z_j, respectively, so it has a thickness $h_j = z_j - z_{j-1}$. The top interface is located at $z_0 = 0$, and the bottom interface is in fact $z_N = \infty$. The continuity conditions require that the three displacement components, (u_x, u_y, u_z) and the three stress components (σ_{zx}, σ_{zy}, σ_{zz}) have to be continuous across interfaces between different layers, i.e.,

$$\lim_{z \uparrow z_j} u_i^j = \lim_{z \downarrow z_j} u_i^{j+1}, \qquad \lim_{z \uparrow z_j} \sigma_{zi}^j = \lim_{z \downarrow z_j} \sigma_{zi}^{j+1}, \qquad i = x, y, z. \tag{13}$$

Next, it turns out to be convenient when we introduce the modified coefficient vectors

$$\boldsymbol{T}^j = \{T_1^j, T_2^j, T_3^j\}^T = \{\overline{T}_1^j e^{i\xi z_{j-1}}, \overline{T}_2^j e^{i\zeta z_{j-1}}, \overline{T}_3^j e^{i\zeta z_{j-1}}\}^T, \tag{14}$$

$$\boldsymbol{R}^j = \{R_1^j, R_2^j, R_3^j\}^T = \{\overline{R}_1^j e^{-i\xi z_j}, \overline{R}_2^j e^{-i\zeta z_j}, \overline{R}_3^j e^{-i\zeta z_j}\}^T. \tag{15}$$

Combining Eqs. (13) – (15) and the elasticity relations (A5) – (A7) given in Appendix A, we obtain the recurrence scheme

$$\boldsymbol{R}^j = [U]_t^j \boldsymbol{R}^{j+1} + [U]_r^j \boldsymbol{T}^j, \tag{16}$$

$$\boldsymbol{T}^{j+1} = [D]_r^j \boldsymbol{R}^{j+1} + [D]_t^j \boldsymbol{T}^j, \tag{17}$$

in which

$$\begin{bmatrix} U_t^j | U_r^j \\ \hline D_r^j | D_t^j \end{bmatrix} = \begin{bmatrix} I_{r1}^j | -I_{t1}^{j+1} \\ \hline I_{r2}^j | -I_{t2}^{j+1} \end{bmatrix}^{-1} \begin{bmatrix} I_{r1}^{j+1} | -I_{t1}^j \\ \hline I_{r2}^{j+1} | -I_{t2}^j \end{bmatrix} \mathrm{diag}(e^{i\xi h_{j+1}}, e^{i\zeta h_{j+1}}, e^{i\zeta h_{j+1}}, e^{i\xi h_j}, e^{i\zeta h_j}, e^{i\zeta h_j}). \tag{18}$$

The *I*-matrices may be found in Eq. (A8) of Appendix A. The matrices $[U]_t^j$, $[U]_r^j$, $[D]_t^j$, and $[D]_r^j$ can be interpreted as the local transmission and reflection matrices for the waves impinging on the jth layer from below and above, as shown in Fig. (1).

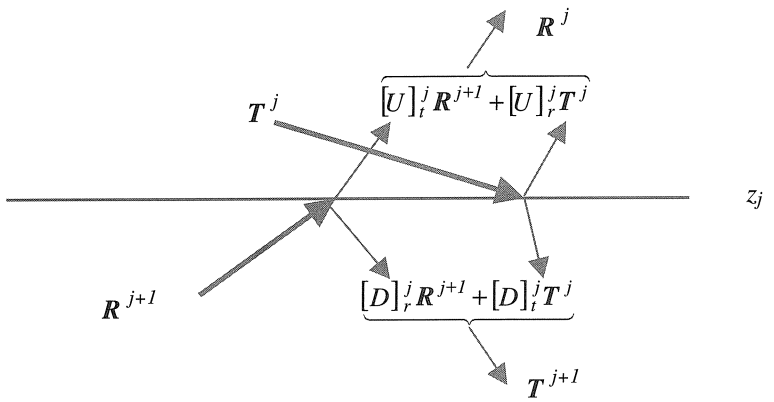

Fig. 1. The physical interpretation of the local transmission and reflection matrices.

It is obvious from Eqs. (16) and (17) that there is an interrelation between the amplitudes of the transmitted and reflected waves of adjacent layers. For example, repeated application Eq. (16) reveals that the amplitudes of the upgoing waves at the first interface may be written as

$$R^1 = [U]_t^1[U]_t^2 \ldots [U]_t^{N-2}[U]_r^{N-1}T^{N-1} + [U]_t^1[U]_t^2 \ldots [U]_t^{N-3}[U]_r^{N-2}T^{N-2} + \ldots + [U]_t^1[U]_r^2T^2 + [U]_r^1T^1. \tag{19}$$

The applied recurrent process stops due to the fact that $R^N = 0$ since no upgoing waves are coming from infinity. From Eq. (17) it follows that T^{N-1}, T^{N-2},..., T^1 are, in turn, functions of R^{N-1}, R^{N-2},..., R^1 and T^0. The latter vector is determined by the boundary conditions at the surface of the medium and involves the action of the source.

As shown in this example, it is not convenient to work with the local transmission and reflection matrices. To relate the transmitted and reflected waves at a specific interface without explicitly referring to the waves at the other interfaces, a global type of reflection and transmission matrices is required, see for example Abdelkarim (1999). These matrices are obtained through some algebraic manipulations with Eqs. (16) and (17). First, use of the radiation condition $R^N = 0$ for $j = N$-1 gives

$$R^{N-1} = [U]_r^{N-1}T^{N-1}, \qquad T^N = [D]_t^{N-1}T^{N-1}, \tag{20}$$

Subsequently substituting the above relations in Eqs. (16) and (17), and repeating this for all interfaces, yields

$$R^j = [B]_u^jT^j, \qquad T^{j+1} = [B]_d^jT^j, \qquad j = 1, \ldots, N-1, \tag{21}$$

in which

$$[B]_u^j = [U]_r^j + [U]_t^j[B]_u^{j+1}[B]_d^j, \qquad [B]_d^j = [I - D_r^jB_u^{j+1}]^{-1}[D]_t^j, \tag{22}$$

where I denotes the unit matrix and

$$[B]_u^{N-1} = [U]_r^{N-1}, \qquad [B]_d^{N-1} = [D]_t^{N-1}. \tag{23}$$

Now the matrices $[B]_u^j$ are the global reflection matrices linking the downgoing waves below an interface with the upgoing waves below the same interface. Similarly, the matrices $[B]_d^j$ are the global transmission matrices linking the downgoing waves below an interface with the downgoing waves above the same interface. Using Eq. (21), R^1 is explicitly related to T^1 only. This is in contrast to the application of Eq. (16), which led to an expression that showed the explicit dependence of R^1 on T^{N-1}, T^{N-2},..., T^1.

4 Numerical integration

The total response to a dynamic loading is the summation of the responses to all its harmonic components. This summation process is carried out using the Fast Fourier Transform. Consider an arbitrary time harmonic loading function $\sigma_{zz}(x, y)e^{-i\omega t}$, defined on the area shown in Fig. (2). Omitting the time variation, the spatial Fourier integral representation of this loading function is

$$\sigma_{zz}(x,y) = \frac{1}{4\pi^2}\int_{-\infty}^{\infty}\int_{-\infty}^{\infty}\sigma_{zz}(\alpha,\beta)e^{i(\alpha x+\beta y)}d\alpha d\beta, \tag{24}$$

where, inversely,

$$\sigma_{zz}(\alpha,\beta) = \int_{-\infty}^{\infty}\int_{-\infty}^{\infty}\sigma_{zz}(x,y)e^{-i(\alpha x+\beta y)}dxdy, \tag{25}$$

For loading functions acting in other directions, expressions similar to Eqs. (24) and (25) can be given. As shown in Fig. (2), there are two areas: the loaded area and the total area. The loaded area represents the actual area where the load is applied. The total area $X_0 \times Y_0$, which includes the loaded area, represents the domain within which the response will be evaluated.
To obtain discrete expressions of Eqs. (24) and (25), we first divide the area $X_0 \times Y_0$ into (M-1) equidistant increments Δx in the x-direction and (N-1) equidistant increments Δy in the y-direction. The load function is then defined on a set of discrete points (x_p, y_q) given by

$$x_p = p\Delta x, \qquad p = 0, \ldots, M-1, \qquad y_q = q\Delta y, \qquad q = 0, \ldots, N-1. \tag{26}$$

The numerical values of the load function at the points outside the loaded area are zero. For an area $X_0 \times Y_0$, the fundamental spatial frequencies in the x and y directions are, respectively,

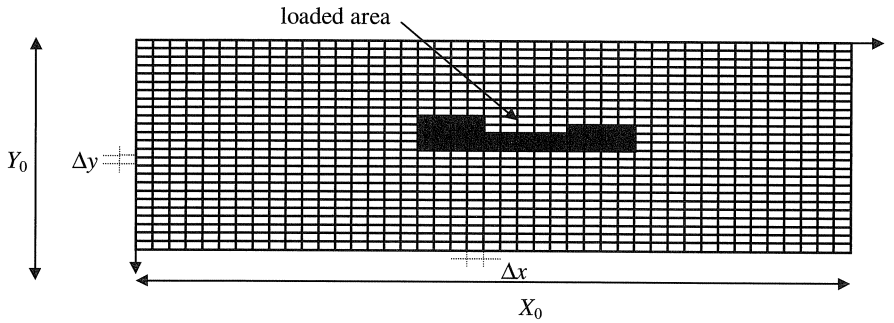

Fig. 2. Arbitrary loading function defined on the total area $X_0 \times Y_0$.

$$\alpha_0 = \frac{2\pi}{X_0}, \qquad \beta_0 = \frac{2\pi}{Y_0}. \tag{27}$$

Second, we replace the continuous wavenumber domain with a discrete one by introducing the discrete wavenumbers

$$\alpha_m = m\alpha_0, \qquad m = -\frac{M}{2}+1, \ldots, \frac{M}{2}, \qquad \beta_n = n\beta_0, \qquad n = -\frac{N}{2}+1, \ldots, \frac{N}{2}. \tag{28}$$

When the above notations are employed, the exponential factor in Eq. (24) takes the discrete form

$$e^{i(\alpha_m x_p + \beta_n y_q)} = e^{i(m\alpha_0 p\Delta x + n\beta_0 q\Delta y)} = e^{2\pi i\left(\frac{mp}{M}+\frac{nq}{N}\right)}. \tag{29}$$

The corresponding discrete expressions of Eqs.(24) and (25) are

$$\sigma_{zz}(x_p, y_q) = \frac{\alpha_0\beta_0}{4\pi^2} \sum_{m=-\frac{M}{2}+1}^{\frac{M}{2}} \sum_{n=-\frac{N}{2}+1}^{\frac{N}{2}} \sigma_{zz}(\alpha_m, \beta_n) e^{2\pi i\left(\frac{mp}{M}+\frac{nq}{N}\right)}, \qquad \begin{matrix} p = 0, 1, \ldots, M-1, \\ q = 0, 1, \ldots, N-1, \end{matrix} \tag{30}$$

$$\sigma_{zz}(\alpha_m, \beta_n) = \Delta x\Delta y \sum_{p=0}^{M-1} \sum_{q=0}^{N-1} \sigma_{zz}(x_p, y_q) e^{-2\pi i\left(\frac{mp}{M}+\frac{nq}{N}\right)}, \qquad \begin{matrix} m = -\frac{M}{2}+1, \ldots, \frac{M}{2}, \\ n = -\frac{N}{2}+1, \ldots, \frac{N}{2}. \end{matrix} \tag{31}$$

Now consider a load function that is represented by Eq. (30). Each term under the summation represents a load component with a harmonic behavior in the x- and y-directions. These components are characterized by the wavenumbers α_m and β_n, respectively, and have an amplitude $\sigma_{zz}(\alpha_m, \beta_n)$. The corresponding amplitudes of the displacement field due to such a loading component can be expressed as

$$\begin{Bmatrix} u_x(\alpha_m, \beta_n) \\ u_y(\alpha_m, \beta_n) \\ u_z(\alpha_m, \beta_n) \end{Bmatrix} = [I_{t1}(\alpha_m, \beta_n) \vdots I_{r1}(\alpha_m, \beta_n)] \begin{Bmatrix} \overline{T}(\alpha_m, \beta_n) \\ \overline{R}(\alpha_m, \beta_n) \end{Bmatrix}. \tag{32}$$

The matrices I_{t1} and I_{r1} are given in Appendix A. The total response in the spatial domain is the superposition of the responses to each loading component $\sigma_{zz}(\alpha_m, \beta_n)$. Then, similarly to Eq. (30), the total response to an arbitrary loading function may be expressed as

$$u_i(x_p, y_q) = \frac{\alpha_0\beta_0}{4\pi^2} \sum_{m=-\frac{M}{2}+1}^{\frac{M}{2}} \sum_{n=-\frac{N}{2}+1}^{\frac{N}{2}} u_i(\alpha_m, \beta_n) e^{2\pi i\left(\frac{mp}{M}+\frac{nq}{N}\right)}, \qquad \begin{matrix} p = 0, 1, \ldots, M-1, \\ q = 0, 1, \ldots, N-1, \end{matrix} \tag{33}$$

where $i = x,y,z$. At this stage it should be noted that the inverse matrix in Eq. (22) will become singular for certain real values of of α and β. These singularities may be associated with phenomena like surface waves (Rayleigh waves) or interface waves (Stoneley waves). To avoid the numerical

difficulties associated with these singularities, we apply a small amount of numerical damping. The idea behind this is to shift the singularities from the real α- and β-axes, so that the discrete integration process in Eq. (33) can be carried out without further difficulties. The only change that is needed for the introduction of the numerical damping consists of modifying the Lamé parameters of the material by multiplying these with the complex factor $(1 - 2i\zeta_s)$, where ζ_s is the damping ratio. In turn, the complex elastic constants affect the wave speeds c_1 and c_2, which will become $c_1^* \approx c_1\sqrt{1 - i\zeta_s}$ and $c_2^* \approx c_2\sqrt{1 - i\zeta_s}$.
When the dynamic loading contains more than one temporal frequency component, the responses due to all different frequency components must be added as well. This is equivalent to determining the inverse of the Fourier transformation in Eq. (5). A similar numerical approach as for the horizontal spatial coordinates may be employed for this.

5 Comparison with the static Boussinesq solution

One of the most common ways of finding the static displacements and static stresses in a homogeneous elastic half-space is to apply the Boussinesq solution from the theory of elasticity. For a vertical point load of force F acting on a homogeneous elastic half-space, the Boussinesq solution for the vertical component of the displacement in the half-space is

$$u_z = \frac{F}{4\pi\mu R}\left(\frac{\lambda + 2\mu}{\lambda + \mu} + \frac{z^2}{R^2}\right), \tag{34}$$

in which $R = \sqrt{x^2 + y^2 + z^2}$ is the distance from the point load to the point of observation. On the surface $z = 0$, the displacement can be written in terms of the modulus of elasticity E and the Poisson ratio ν as

$$u_z = \frac{F(1 - \nu^2)}{\pi E R}. \tag{35}$$

Now we will compare the amplitude of an approximately static vertical displacement obtained by the present method with the static vertical displacement following from the above relation.
The former vertical displacement results from a vertical time-harmonic point load with a very small frequency $f = 0.01$ Hz. In both cases the applied vertical point load has a force $F = 10^8$ N.
The considered homogeneous half-space is characterized by a modulus of elasticity $E = 10^8$ N/m^2, a Poisson ratio $\nu = 0.25$, and a mass density $\rho = 2000$ kg/m^3. Further we employ a numerical damping ratio $\zeta_s = 0.01$. From Fig. (3) it is obvious that the agreement between our approximate solution and the exact Boussinesq solution is good.

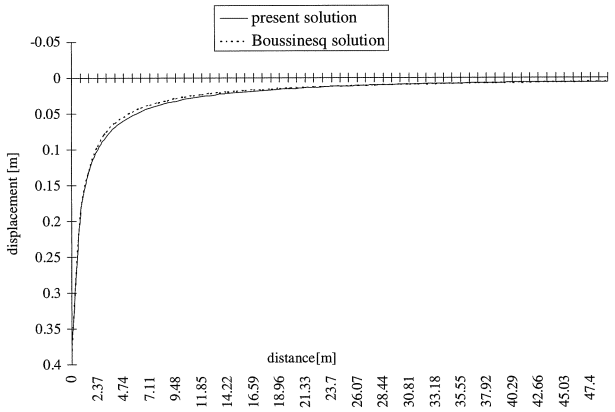

Fig. 3. *A comparison between our approximately static vertical displacement and the Boussinesq exact static vertical displacement.*

6 Comparison with the dynamic Lamb solution

The classical analysis of waves being generated by time-harmonic line loads or point loads located on the surface of a half-space has been performed by Lamb (1904). Superposition techniques were used to obtain results for pulse loading. Here we will consider the case of a time-harmonic vertical point load acting on a homogeneous half-space. The main difficulty of Lamb's problem is to evaluate the infinite integrals appearing in the solution of the wave equations. In Lamb's solution, a free surface wave may be distinguished in addition to the usual compressional wave and shear wave. This free surface wave is called the Rayleigh wave, and it corresponds to a pole appearing in the integrand. Lamb found that at a great horizontal distance from the source the most important part of the displacement is associated with this Rayleigh wave. In the frequency domain, the Rayleigh wave part of the vertical surface displacement due to a vertical point source of force F is approximately equal to

$$u_z(r, \omega) = \frac{\kappa F}{2\mu} K \sqrt{\frac{2}{\pi \kappa r}} e^{i\left(\kappa r + \frac{\pi}{4}\right)}, \tag{36}$$

in which $\kappa = \omega / c_r$, where c_r is the velocity of the Rayleigh wave. For a Poisson ratio of 0.25, the value of K is 0.18349 [see Lamb (1904), p.18].

Here we will compare the amplitude of the harmonic vertical displacement as obtained by the present method with the one following from the approximate solution given above. At first sight this may seem impossible, since the present method does not allow the separation of the Rayleigh wave contribution from the compressional and shear wave contributions. However, it turns out that the latter are relatively small when the horizontal distance r is larger than several times the wave-length of the Rayleigh wave. For these values of r it makes sense to compare the frequency domain results from the present method with those given by Eq. (36).

With the present method, the frequency domain results follow from a two-dimensional inverse Fourier transformation whose discrete form is given in Eq. (33). In this specific case we have, according to Appendix A,

$$u_z(\alpha_m, \beta_n) = (i\xi \; -i\beta \; i\alpha)\begin{Bmatrix} T_1(\alpha_m, \beta_n) \\ T_2(\alpha_m, \beta_n) \\ T_3(\alpha_m, \beta_n) \end{Bmatrix}, \tag{37}$$

in which the boundary conditions at the surface require that

$$\begin{Bmatrix} T_1(\alpha_m, \beta_n) \\ T_2(\alpha_m, \beta_n) \\ T_3(\alpha_m, \beta_n) \end{Bmatrix} = \mu^{-1}\begin{bmatrix} \gamma^2 & 2\beta\zeta & -2\alpha\zeta \\ -2\alpha\xi & 2\alpha\beta & k_2^2 - 2\alpha^2 \\ -2\beta\xi & 2\beta^2 - k_2^2 & -2\alpha\beta \end{bmatrix}^{-1}\begin{Bmatrix} -F \\ 0 \\ 0 \end{Bmatrix}, \tag{38}$$

where $\gamma^2 = 2\alpha^2 + 2\beta^2 - k_2^2$ and F is the spatial Fourier transform of the frequency domain vertical point load $F\delta(x)\delta(y)$. To obtain an accurate numerical result, X_0, Y_0, M, and N must be sufficiently large. To analyze the situation, consider the case $\beta = 0$. In the complex α-plane, the Rayleigh poles, in the presence of the numerical damping, are located at

$$\pm\alpha_r = \frac{\omega}{c_r^*} \approx \frac{\omega}{c_r(1 - i\zeta_s)} \approx \frac{\omega}{c_r}(1 + i\zeta_s). \tag{39}$$

The distance from these poles to the integration path of the inverse Fourier transformation, i.e. the real α-axis, is equal to $\omega\zeta_s / c_r$. To obtain accurate results, the distance between the sampling points on the real α-axis should be much less than the latter value, so

$$\alpha_0 = \frac{2\pi}{X_0} << \frac{2\pi f \zeta_s}{c_r}, \tag{40}$$

and thus the requirement is

$$X_0 >> \frac{c_r}{f\zeta_s}. \tag{41}$$

Further, a truncation of the inverse Fourier integral should take place far away from the poles, which means that in the discrete case

$$\frac{M}{2}\alpha_0 = \frac{\pi M}{X_0} >> \frac{\omega}{c_r} = \frac{2\pi f}{c_r}, \tag{42}$$

so another requirement is

$$M >> \frac{2fX_0}{c_r}. \tag{43}$$

Equivalent inequalities may be found for Y_0 and N by considering the case $\alpha = 0$.
For purpose of comparison, we again consider a homogeneous half-space characterized by a modulus of elasticity $E = 10^8$ N/m^2, a Poisson ratio $\nu = 0.25$, a mass density $\rho = 2000$ kg/m^3, and a

numerical damping ratio $\zeta_s = 0.01$. The surface of this half-space is subjected to a harmonic vertical point load with an amplitude $F = 10^5$ N, and a frequency $f = 1$ Hz. The origin of the coordinate system is chosen to coincide with the location of the point load, as shown in Fig. (4). For this configuration it turns out that the requirements on X_0, Y_0, M, and N are

$$X_0 >> 13000, \qquad Y_0 >> 13000, \tag{44}$$

say $X_0 = Y_0 = 32$ km, and consequently

$$M >> 493, \qquad N >> 493, \tag{45}$$

say $M = N = 1024$.

From these values of M and N it is obvious that an accurate evaluation of the inverse Fourier transformation in Eq. (33) will require a fast computer with a large working memory. Nowadays the numerical evaluations of this kind are very well possible, however. The obtained results are in good agreement with those following from Lamb's approximation, as may be seen in Fig. (5). The numerical damping is responsible for the faster decrease of the amplitude with the present method. On PC with a 450 MHz Pentium processor, the generation of each figure takes 620 s.

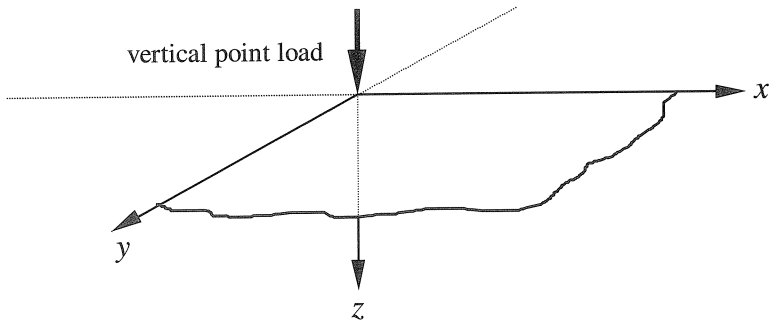

Fig. 4. A half-space subjected to a harmonic vertical point load.

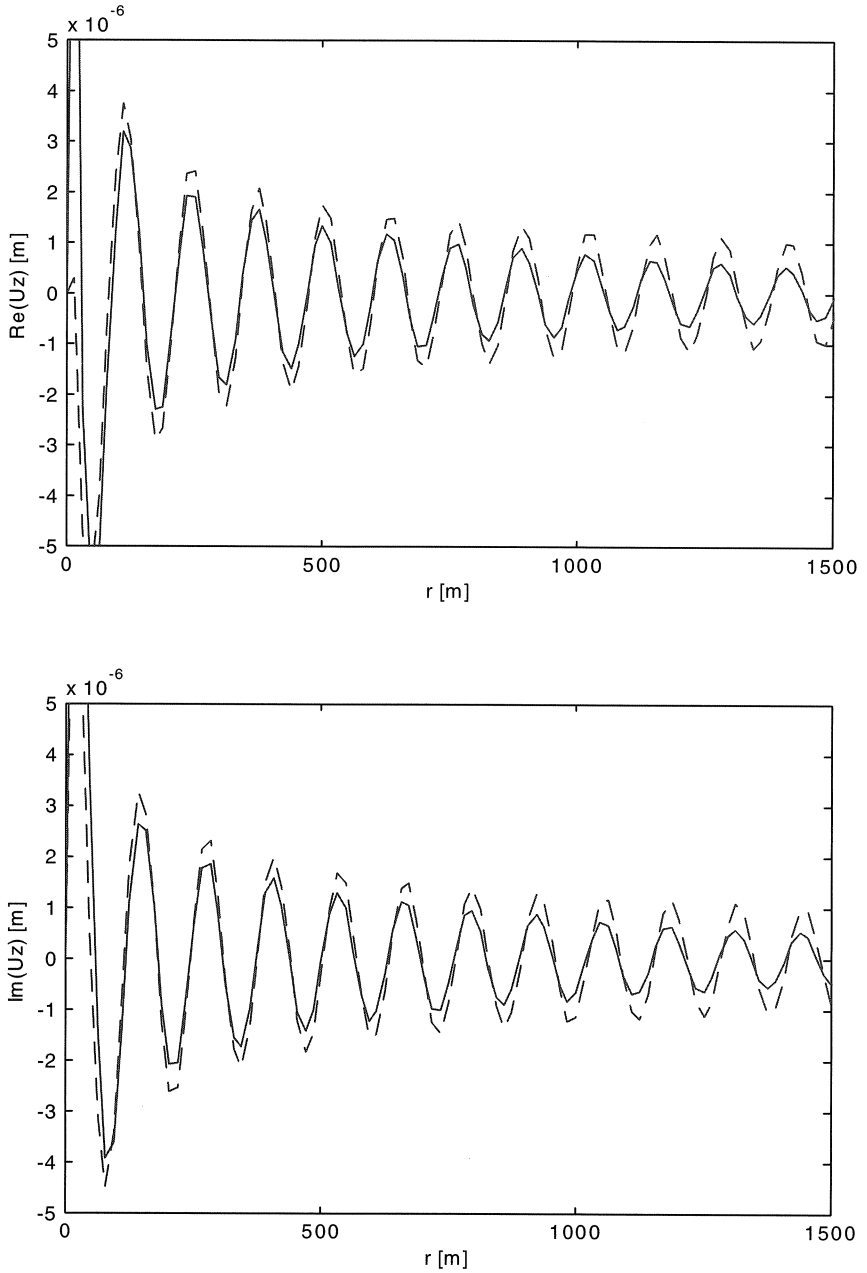

Fig. 5. *A comparison between the frequency-domain vertical displacement $u_z(x,y,z,\omega)$ following from the present method (solid lines) and Lamb's solution (dotted lines). The real part of $u_z(x,y,z,\omega)$ is shown above, and the imaginary part of $u_z(x,y,z,\omega)$ is shown below. Here, $z = 0$ so $r = \sqrt{x^2 + y^2}$ indicates the distance from the point load to the point of observation.*

7 Conclusions

A mathematically straightforward method for the evaluation of the dynamic response of a layered half-space subjected to a surface load has been presented. The three-dimensional wave propagation problem has been solved by first transforming the problem to the wavenumber-frequency domain, then solving the corresponding problem, and finally applying the relevant inverse transformations. In this way, the stresses and displacements may be calculated at any point within the layered elastic half-space.

The evaluation of the wave field quantities only requires a commonly available Fast Fourier Transformation routine. Difficulties due to the singularities in the wavenumber-frequency domain have been avoided by introducing a small amount of numerical damping. All types of waves are automatically included in the solution. Tests have been performed for two canonical situations. First, an almost static response has been evaluated and compared with the Boussinesq solution. Second, a harmonic response has been determined and compared with the far-field approximation of Lamb's solution. Both tests show a good agreement between the results obtained by the present method and the results that follow from the mentioned solutions.

Appendix A

In this appendix, a summary of the basic elastic equations in a Cartesian coordinate system is presented. To start with, the relations between the components of the strain tensor ε and the displacement vector u are

$$\varepsilon_{xx} = \frac{\partial u_x}{\partial x}, \qquad \varepsilon_{yy} = \frac{\partial u_y}{\partial y}, \qquad \varepsilon_{zz} = \frac{\partial u_z}{\partial z},$$

$$2\varepsilon_{xy} = 2\varepsilon_{yx} = \frac{\partial u_x}{\partial y} + \frac{\partial u_y}{\partial x}, \qquad 2\varepsilon_{yz} = 2\varepsilon_{zy} = \frac{\partial u_y}{\partial z} + \frac{\partial u_z}{\partial y}, \qquad 2\varepsilon_{zx} = 2\varepsilon_{xz} = \frac{\partial u_z}{\partial x} + \frac{\partial u_x}{\partial z}. \tag{A1}$$

Substituting this in Hooke's law for an isotropic elastic medium, the following relations between the components of the stress tensor σ and the displacement vector u are obtained

$$\sigma_{xx} = \lambda\left(\frac{\partial u_x}{\partial x} + \frac{\partial u_y}{\partial y} + \frac{\partial u_z}{\partial z}\right) + 2\mu\frac{\partial u_x}{\partial x},$$

$$\sigma_{yy} = \lambda\left(\frac{\partial u_x}{\partial x} + \frac{\partial u_y}{\partial y} + \frac{\partial u_z}{\partial z}\right) + 2\mu\frac{\partial u_y}{\partial y},$$

$$\sigma_{zz} = \lambda\left(\frac{\partial u_x}{\partial x} + \frac{\partial u_y}{\partial y} + \frac{\partial u_z}{\partial z}\right) + 2\mu\frac{\partial u_z}{\partial z},$$

$$\sigma_{xy} = \sigma_{yx} = \mu\left(\frac{\partial u_x}{\partial y} + \frac{\partial u_y}{\partial x}\right), \qquad \sigma_{yz} = \sigma_{zy} = \mu\left(\frac{\partial u_y}{\partial z} + \frac{\partial u_z}{\partial y}\right), \qquad \sigma_{zx} = \sigma_{xz} = \mu\left(\frac{\partial u_z}{\partial x} + \frac{\partial u_x}{\partial z}\right). \tag{A2}$$

According to Eq. (2) of the main text, the relations between the components of the displacement vector $\boldsymbol{u}$ and the scalar and vector potentials ϕ and Ψ are

$$u_x = \frac{\partial \phi}{\partial x} + \frac{\partial \Psi_z}{\partial y} - \frac{\partial \Psi_y}{\partial z}, \qquad u_y = \frac{\partial \phi}{\partial y} + \frac{\partial \Psi_z}{\partial x} - \frac{\partial \Psi_x}{\partial z}, \qquad u_z = \frac{\partial \phi}{\partial z} + \frac{\partial \Psi_y}{\partial x} - \frac{\partial \Psi_x}{\partial y}. \tag{A3}$$

Substitution of Eq. (A3) into Eq. (A2) yields the stress components in terms of the scalar and vector potentials. For the stress components that are relevant to the theory in main text, the relations are

$$\sigma_{zx} = \mu\left(2\frac{\partial^2 \phi}{\partial x \partial z} + \frac{\partial}{\partial z}\left(\frac{\partial \Psi_z}{\partial y} - \frac{\partial \Psi_y}{\partial z}\right) + \frac{\partial}{\partial x}\left(\frac{\partial \Psi_y}{\partial x} - \frac{\partial \Psi_x}{\partial y}\right)\right),$$

$$\sigma_{zy} = \mu\left(2\frac{\partial^2 \phi}{\partial y \partial z} - \frac{\partial}{\partial z}\left(\frac{\partial \Psi_z}{\partial x} - \frac{\partial \Psi_x}{\partial z}\right) + \frac{\partial}{\partial y}\left(\frac{\partial \Psi_y}{\partial x} - \frac{\partial \Psi_x}{\partial y}\right)\right),$$

$$\sigma_{zz} = \lambda \nabla^2 \phi + 2\mu\left(\frac{\partial^2 \phi}{\partial z^2} + \frac{\partial}{\partial z}\left(\frac{\partial \Psi_y}{\partial x} - \frac{\partial \Psi_x}{\partial y}\right)\right). \tag{A4}$$

Substitution of the potential components of Eqs. (7) – (10) into Eqs. (A3) and (A4) yields the following matrix expression for the displacement and the relevant stress components

$$\begin{Bmatrix} \boldsymbol{u} \\ \boldsymbol{\sigma} \end{Bmatrix} = \begin{bmatrix} I_{t1} & I_{r1} \\ I_{t2} & I_{r2} \end{bmatrix} \begin{Bmatrix} W^d \\ W^u \end{Bmatrix}, \tag{A5}$$

where

$$\boldsymbol{u} = \begin{Bmatrix} u_x \\ u_y \\ u_z \end{Bmatrix}, \qquad \sigma = \begin{Bmatrix} \sigma_{zx} \\ \sigma_{zy} \\ \sigma_{zz} \end{Bmatrix}. \tag{A6}$$

$$W^d = e^{i(\alpha x + \beta y - \omega t)} \begin{Bmatrix} T_1 e^{i\xi z} \\ T_2 e^{i\zeta z} \\ T_3 e^{i\zeta z} \end{Bmatrix}, \qquad W^u = e^{i(\alpha x + \beta y - \omega t)} \begin{Bmatrix} R_1 e^{-i\xi z} \\ R_2 e^{-i\zeta z} \\ R_3 e^{-i\zeta z} \end{Bmatrix}, \tag{A7}$$

and

$$[I]_{t1} = \begin{bmatrix} i\alpha & -\frac{i\alpha\beta}{\zeta} & -\frac{i}{\zeta}(\beta^2 + \zeta^2) \\ i\beta & \frac{i}{\zeta}(\alpha^2 + \zeta^2) & \frac{i\alpha\beta}{\zeta} \\ i\xi & -i\beta & i\alpha \end{bmatrix}, \qquad [I]_{r1} = \begin{bmatrix} i\alpha & \frac{i\alpha\beta}{\zeta} & \frac{i}{\zeta}(\beta^2 + \zeta^2) \\ i\beta & -\frac{i}{\zeta}(\alpha^2 + \zeta^2) & -\frac{i\alpha\beta}{\zeta} \\ -i\xi & -i\beta & i\alpha \end{bmatrix},$$

$$[I]_{t2} = \mu \begin{bmatrix} \gamma^2 & 2\beta\zeta & -2\alpha\zeta \\ -2\alpha\xi & 2\alpha\beta & k_2^2 - 2\alpha^2 \\ -2\beta\xi & 2\beta^2 - k_2^2 & -2\alpha\beta \end{bmatrix}, \qquad [I]_{r2} = \mu \begin{bmatrix} \gamma^2 & -2\beta\zeta & 2\alpha\zeta \\ 2\alpha\xi & 2\alpha\beta & k_2^2 - 2\alpha^2 \\ 2\beta\xi & 2\beta^2 - k_2^2 & -2\alpha\beta \end{bmatrix}, \tag{A8}$$

with

$$\gamma^2 = 2\alpha^2 + 2\beta^2 - k_2^2. \tag{A9}$$

References

ABDELKARIM, A.M.A.M. (1999). "Dynamic response of an elastic layered half-space", Ph.D. thesis, Delft University of Technology, Delft, The Netherlands.

CAGNIARD, L. (1939). *Réflection et réfraction des ondes seismiques progressives*. Gauthier-Villars, Paris (in French).

CHAPMAN, C.H. (1978). "A new method for computing synthetic seismograms", Geophys. J. R. Astr. Soc. **46**.

DE HOOP, A.T. (1960). *A modification of Cagniard's method for solving seismic pulse problems*, Appl. Sci. Res. **B8**.

DE HOOP, A.T. (1988). "Acoustic radiation from impulsive sources in a layered fluid", Nieuw Archief voor Wiskunde **6**.

DUNKIN, J.W. (1965). "Computation of modal solutions in layered elastic media at high frequencies", Bull. Seism. Soc. Am. **55**.

EWING, W.M., JARDETZKY, W.S., and PRESS, F. (1957). *Elastic waves in layered media*, McGraw-Hill, New York.

ERINGEN, A.C., and SUHUBI, E.S. (1975). *Elastodynamics II, Linear theory*, Academic Press, New York.

GILBERT, F., and BACKUS, G.E. (1966). "Propagator matrices in elastic wave and vibration problems", Geophysics **31**.

HARKRIDER, D.G. (1964). "Surface waves in multilayered elastic media, part I. Rayleigh and Love waves from buried sources in a multilayered elastic half-space", Bull. Seism. Soc. Am. **54**.

HARKRIDER, D.G. (1970). "Surface waves in multilayered elastic media, part II. Higher mode spectra and spectral ratios from point sources in plane layered earth models", Bull. Seism. Soc. Am. **60**.

HASKELL, N.A. (1953). "The dispersion of surface waves in multilayered media", Bull. Seism. Soc. Am. **43**.

HASKELL, N.A. (1964). "Radiation pattern of surface waves from point source in a multilayered medium", Bull. Seism. Soc. Am. **54**.

HUDSON, J.A. (1969). "A quantitative evaluation of a seismic signal at teleseismic distance, II Body waves and surface waves from an extended source", Geophys. J. R. Astr. Soc. **18**.

KAUSEL, E., and ROESSET (1981). "Stiffness matrices for layered soils", Bull. Seism. Soc. Am. **71**.

KENNETT, B.L.N. (1983). *Seismic wave propagation in stratified media*, Cambridge Univ. Press, Cambridge, England.

LAMB, H. (1904). "On the propagation of tremors over the surface of an elastic solid", Phil. Trans. R. Soc. London, Series A203.

RICHARD, F.E. Jr., HALL, J.R., and WOODS, R.D. (1970). *Vibration of soils and foundations*, Prentice-Hall, Englewood Cliffs, New Jersey.

THOMSON, W.T. (1950). "Transmission of elastic waves through a stratified solid medium", J. Appl. Phys. **21**.

VAN DER HIJDEN, J.H.M.T. (1987). *Propagation of transient elastic waves in stratified anisotropic media,* North-Holland, Amsterdam.

VERWEIJ, M.D., and DE HOOP, A.T. (1990). "Determination of seismic wavefields in arbitrarily continuously layered media using the modified Cagniard method", Geophys. J. Int. **103**.

WOLF, J.P. (1985). *Dynamic soil-structure interaction,* Prentice-Hall, Englewood Cliffs, New Jersey.

WOLF, J.P. (1988). *Soil-structure interaction analysis in time domain,* Prentice-Hall, Englewood Cliffs, New Jersey.